

# Time-Delay Interferometry with optical frequency comb

Massimo Tinto\* and Nan Yu†

*Jet Propulsion Laboratory, California Institute of Technology, Pasadena, CA 91109*

(Dated: October 8, 2018)

## Abstract

Heterodyne laser phase measurements in a space-based gravitational wave interferometer are degraded by the phase fluctuations of the onboard clocks, resulting in unacceptable sensitivity performance levels of the interferometric data. In order to calibrate out the clock phase noises it has been previously suggested that additional inter-spacecraft phase measurements must be performed by modulating the laser beams. This technique, however, considerably increases system complexity and probability of subsystem failure.

With the advent of self-referenced optical frequency combs, it is possible to generate the heterodyne microwave signal that is coherently referenced to the onboard laser. We show in this case that the microwave noise can be cancelled directly by applying modified second-generation Time-Delay Interferometric combinations to the heterodyne phase measurements. This approach avoids use of modulated laser beams as well as the need of additional ultra-stable oscillator clocks.

PACS numbers: 04.80.Nn, 95.55.Ym, 07.60.Ly

---

\*Electronic address: Massimo.Tinto@jpl.nasa.gov

†Electronic address: Nan.Yu@jpl.nasa.gov

## I. INTRODUCTION

Gravitational waves (GWs) are predicted by Einstein's theory of general relativity and represent disturbances of space-time propagating at the speed of light. Because of their extremely small amplitudes and interaction cross-sections, GWs carry information about regions of the Universe that would be otherwise unobtainable through the electromagnetic spectrum. Once detected, GWs will allow us to open a new observational window to the Universe, and perform a unique test of general relativity [1].

Since the first pioneering experiments by Joseph Weber in the early sixties [2], several experimental groups around the world have been attempting to detect GWs. The coming on-line of next-generation gravitational wave interferometers [3, 4], however, is likely to break this sequence of experimental drawbacks and result into the first detection before the end of the current decade.

Contrary to ground-based detectors, which are sensitive to gravitational waves in a band from about a few tens of Hz to a few kilohertz, space-based interferometers are expected to access the frequency region from a few tenths of millihertz to about a few tens of Hz, where GW signals are expected to be larger in number and characterized by larger amplitudes. The most notable example of a space interferometer, which for several decades has been jointly studied in Europe and in the United States of America, is the Laser Interferometer Space Antenna (LISA) mission [5]. By relying on coherent laser beams exchanged among three remote spacecraft along the arms of their forming giant (almost) equilateral triangle of arm-length equal to  $5 \times 10^6$  km, LISA aims to detect and study cosmic gravitational waves in the  $10^{-4} - 1$  Hz band.

A space-based laser interferometer detector of gravitational waves measures relative frequency changes experienced by coherent laser beams exchanged by three pairs of spacecraft. As the laser beams are received, they are made to interfere with the outgoing laser light. Since the received and receiving frequencies of the laser beams can be different by tens to perhaps hundreds of MHz (consequence of the Doppler effect from the relative inter-spacecraft velocities and the intrinsic frequency differences of the lasers), to remove these large beat-notes present in the heterodyne measurements one relies on the use of a microwave signal generated by an onboard clock (usually referred to as Ultra-Stable Oscillator (USO)). The magnitude of the frequency fluctuations introduced by the USO into the het-

erodyne measurements depends linearly on the USOs' noises themselves and the heterodyne beat-note frequencies determined by the inter-spacecraft relative velocities. Space-qualified, state of the art clocks are oven-stabilized crystals characterized by an Allan deviation of  $\sigma_A \approx 10^{-13}$  for averaging times of 1 – 1000 s, covering most of the frequency band of interest to space-based interferometers [5–7]. In the case of the LISA mission, in particular, it was estimated [8] that the magnitude of the power spectral density of the USO's relative frequency fluctuations appearing, for instance, in the unequal-arm Michelson Time-Delay Interferometry (TDI) combination  $X$  would be about six orders of magnitude larger than those due to the residual (optical path and proof-mass) noise sources.

A technique for removing the USO noise from the TDI combinations was devised (see [8–10] for more details). This technique requires the modulation of the laser beams exchanged by the spacecraft, and the further measurement of six more inter-spacecraft relative phases by comparing the sidebands of the received beam against sidebands of the transmitted beam. The physical reason behind the use of modulated beams for calibrating the USOs noises is to exchange the USOs phase fluctuations with the same time delay as their lasers among the three spacecraft by performing side-bands/side-bands measurements [8–10]. In so doing, additional six phase measurements are generated that allow one to calibrate out the USOs phase fluctuations from the TDI combinations while preserving the gravitational wave signal in the resulting USO-calibrated TDI data.

It should be noticed, however, that if we could coherently transfer the laser phase fluctuations to the microwave signal used in the heterodyne measurements, then we would need to cancel only one noise (the laser noise), which might be possible by deriving some new TDI combinations. Coherently linking optical laser frequencies to microwave frequencies has been thought to be impossible because of the inability to directly count the optical frequency of a laser. However, with the recent advent of the self-referenced octave-span optical frequency comb (OFC) scheme (for which Hall [11] and Hänsch [12] received the physics Nobel Prize in 2005) it is now possible to generate a microwave frequency signal that is coherent to the frequency of the laser at a level significantly better than the frequency stability required of a USO to avoid the modulation-driven USO noise calibration procedure.

Although most of the reported implementations of the self-referenced frequency comb technique have been performed in a laboratory environment, active developments are being made for space-qualified OFC systems [13, 14]. In addition, more recent micro comb source

developments promise much smaller and integratable comb devices [15]. If each spacecraft could then generate heterodyne measurements by relying on the OFC technique, then the question to be answered is whether there exist new TDI combinations that could account for the modified laser noise transfer functions into the heterodyne measurements. The answer to this question is yes, and in what follows we will derive their expressions.

In Section II we give a brief summary of the OFC technique, and of characteristics of a self-referenced comb. In Section III we then exemplify through a simple interferometric configuration illustrating how the “USO noise” can be canceled with TDI when the OFC technique is implemented. In the same section we then move on to the realistic configuration of a space-based interferometer (such as LISA) and derive the expressions for the twelve inter-spacecraft heterodyne phase measurements when the OFC technique is used. This allows us to obtain the new second-generation (i.e. flex-free) TDI combinations [16–19] that simultaneously cancel the laser and the comb-generated microwave signal phase noises. In Section IV we finally present our concluding remarks, and emphasize that the use of the OFC technique will result into a hardware and system design simplification, and increase system reliability of future space-based gravitational wave interferometers.

## II. THE OPTICAL FREQUENCY COMB TECHNIQUE

An OFC is a set of narrow spectral lines equally spaced in the frequency domain. More importantly, when all the comb lines are phase coherent (i.e. have fixed phase relationship) the superposition of all the comb lines manifest themselves as a periodical wave train in the time domain. The resulting repetition rate is equal to the comb spacing and it is governed by the Fourier transform relationship. More often, the comb lines are in phase so the time domain waveform is a train of short pulses separated by the inverse of the repetition rate. The pulse width is then Fourier transform limited by the comb spectral width.

Typical OFCs are generated by mode-locked lasers in which multiple modes are locked in phase, outputting short pulse trains. The pulse train propagates with a group velocity while the underline optical carrier travels at the phase velocity. When the modes are exactly in phase, the peak of the carrier is aligned with the peak of the pulse envelope, as shown in the first pulse in figure 1. In the absence of any dispersion, this relationship holds over time as the pulse propagates. In practice, dispersion changes the relative phases of the modes,

and the peak of the carrier amplitude shifts from that of the pulse envelope. This offset is typically referred to as Carrier Envelope Offset (CEO) phase shift and the rate of this offset phase change over a period gives the CEO frequency [20], as shown in the frequency domain spectrum in figure 1. In particular, this implies the well known mode frequency relation:  $f_m = f_{ceo} + mf_{rep}$ . Since  $f_{ceo}$  is affected by dispersion, as there are many environmental effects influencing it,  $f_{ceo}$  is not a stable parameter and, as a consequence, there is no fixed frequency or phase relationship between the optical carrier and the pulse envelope, i.e. the beat-note of the rf signals among the modes. For many years before the recent self-referenced OFC development, the two frequencies were kept separate and used independently.

Recent advancements in the study of ultra-fast phenomena and the field of optical frequency metrology have revolutionized the use of OFC with abilities to measure and control the CEO. As shown in reference [20], if one compares the  $N_m$ th harmonic of the  $m$ th mode with the  $N_{m'}$ th harmonic of the  $m'$ th mode, the beat note of the two yields  $(N_m - N_{m'})f_{ceo}$ . In particular, if the comb has an octave spanning width where one can choose  $N_m = 2$  and  $N_{m'} = 1$ , the mixing beat-note of 1f-2f directly gives the measure of the CEO frequency. Like in a typical phase locking loop, the measured CEO phase can be used to stabilize the CEO itself, resulting in an OFC that has the well-defined relationship between the optical frequencies  $f_m$  in the modes and the rf frequency of the repetition rate  $f_{rep}$ , now referred to as *self-referencing* [21]. Such control capability not only allows one to align carrier amplitude peaks with the short pulse envelopes in ultrafast phenomena study, but more revolutionarily provides the optical frequency divider ability down to microwave in one simple step. In the latter case with a self-referenced comb, what it means is that the optical field in the comb has a coherent phase relationship with its rf beat-note signal and one can count the optical frequency by counting the rf frequency. Furthermore, the optical phase noise is also directly down converted to the rf phase noise. Recent studies have shown that the comb frequency precision can be at  $1 \times 10^{-19}$  [22] while the CEO phase can be controlled down to the mrad level. In the context of the investigation in this paper, the properties of the phase coherent optical divider are exploited for the onboard clock phase noise cancellation and for the generation of stable onboard rf signals directly from the comb.

The most mature self-referenced OFCs are generated with a combination of femtosecond mode locked laser and super-continuum generation to achieve octave spanning spectrum width. While both Ti:Sapphire and fiber mode locked lasers are successfully implemented for

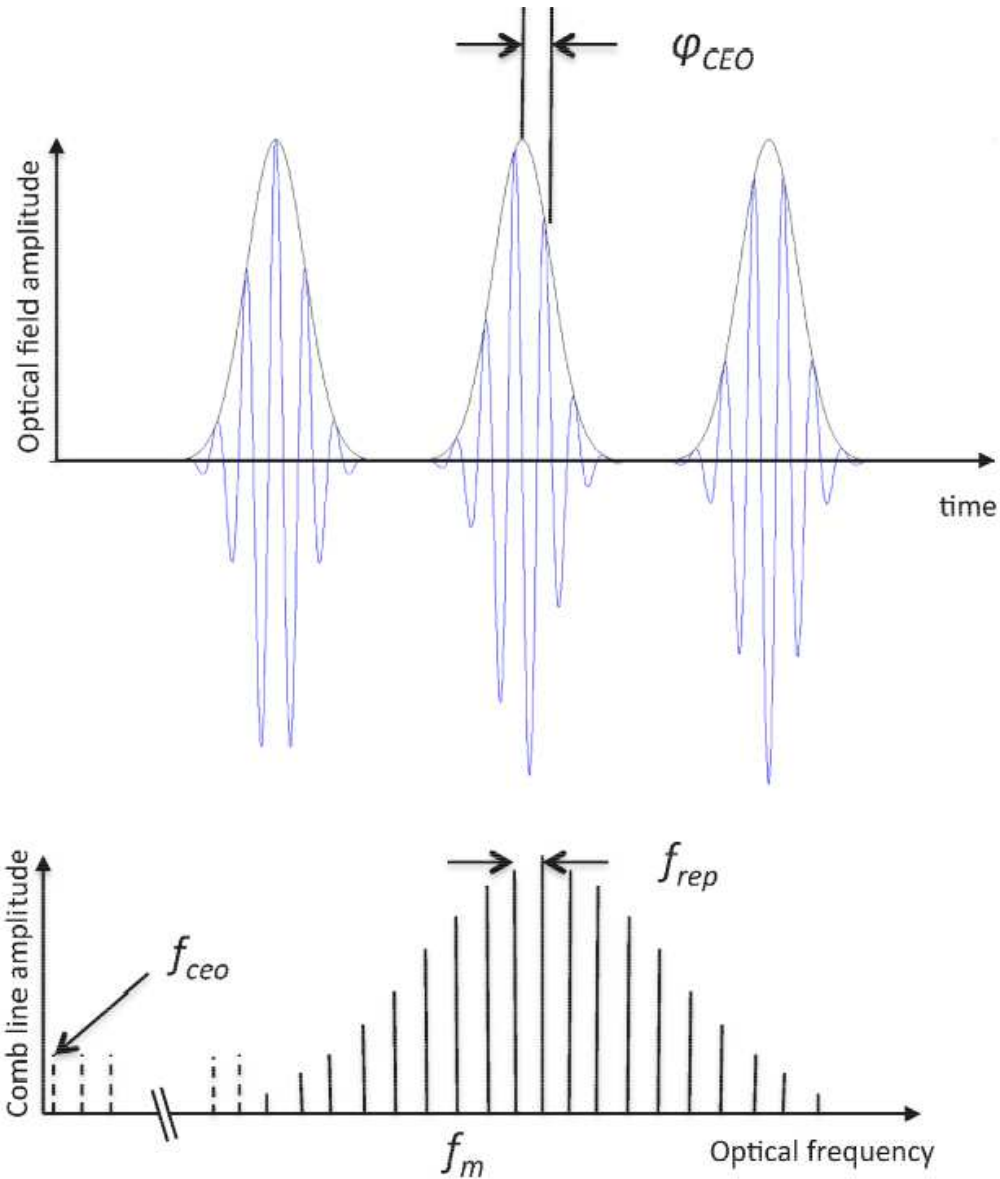


FIG. 1: Illustration of a mode locked laser pulse train and its corresponding comb in the frequency domain. The top plot in the time domain shows the carrier envelope offset phase and its changes. The bottom plot shows the comb lines and the carrier envelope offset frequency near the DC frequency.

self referencing, the most suitable laser source for space interferometer mission may be fiber laser based systems. In fact, self-referencing comb systems are now commercially available, mostly for laboratory applications. Efforts are being made in developing the fiber OFC technology for space applications. A flight OFC system is being developed for sounding

rocket experiments [13], and a femtosecond fiber laser has already been flown in space [14]. It is in fact expected that a flight OFC system, suitable for space missions, will become available in the near future.

More recently it has been shown that coherent OFC can also be generated using high-Q micro resonators through Kerr nonlinear four wave mixing process [23]. In this case, a cw laser is resonantly injected into the resonator and strongly confined in the small volume mode. The high Q-factor leads further field buildup in the resonator, which enhances the Kerr nonlinear effect in the micro resonator. Various cavity eigenmodes can, therefore, be excited through four-wave mixing as the laser light sequentially cascades from the pump to the other modes [24], forming an optical comb with spacing determined by the resonator mode space, free spectral range. When the condition is right, these modes are phase locked in a soliton form, very much like a typical mode locked laser [25]. In comparison with their mode-locked lasers counterparts, however, these whispering gallery mode optical frequency comb generators are characterized by a significantly reduced size and power consumption, along with a high repetition rate. They are, therefore, particularly suitable for miniaturization, chip integration, and space applications. For the purpose of self-referencing in optical metrology, it is important that the comb spans over one octave for 1f-2f self-reference, or at least 2/3 of an octave for 2f-3f self-referencing. While self-referenced micro comb are still been developed in research labs, we believe space-qualified, compact Kerr combs will be available in the near future.

The striking property of the self-referenced OFC is the phase coherence between the optical carriers and their rf beat note signal. As it will be shown later, this allows the laser and resulting microwave signal phase noises cancellation elegantly in the generalized TDI combinations. Furthermore, one can take advantage of the onboard frequency stabilized laser system to generate a stable microwave signal. Since the onboard stabilized lasers are expected to achieve a stability at the level of  $10^{-14}/\sqrt{Hz}$  or better over the frequency range of interests to space interferometer gravitational wave detection, by phase-locking the optical frequency comb to the stabilized laser, the corresponding rf beat-note stability will be also of a few parts in  $10^{14}$ . Therefore, the stabilized OFC technique will provide an rf signal that can be significantly more stable of the current best space-qualified USOs. The OFC implementation will not only eliminate the need for separate USOs but also remove entirely the need for modulated beams used by the USO calibration method, as it will be shown in

the following sections.

### III. TIME-DELAY INTERFEROMETRY WITH OPTICAL FREQUENCY COMB

In the following subsections we derive the modified expressions of the second-generation [16, 18, 19] TDI combinations that simultaneously cancel the laser and the microwave phase noises when the OFC technique is implemented. To physically understand how this is possible, we will first consider a simple interferometer configuration in which the rate-of-changes of the arm-lengths are large enough to require the removal of the beat-notes from the two-way data but small enough to treat the arm-lengths as constant. This will allow us to establish the basis for then deriving new second-generation TDI combinations that a three-arms, six laser links space-based interferometer can generate.

#### A. TDI with OFC: an example application

Let us consider the following idealized unequal-arm interferometer whose end-mirrors are moving with velocities  $V_1$  and  $V_2$  along the directions of arms 1 and 2 respectively (see figure 2). These velocities are relative to the inertial reference frame in which the laser and the beam-splitters are at rest. The two light beams coming out of the two arms are not made to interfere at a common photodetector as each is made to interfere with the incoming light from the laser at a photodetector. This is because direct recombination of the beams at a single photodetector would not suppress the laser phase noise in the phase difference measurement due to the inequality of the arms. <sup>1</sup>

The velocities of the mirrors can be assumed to have frequency components that are outside the band of operation of the interferometer, while their amplitudes are such as to require the use of a numerically controlled oscillator (NCO) (driven by a clock) to remove the beat-notes in the two “two-way” heterodyne phase measurements,  $\phi_1(t)$  and  $\phi_2(t)$ . As a

---

<sup>1</sup> By using two independent photodetectors we decouple the phase fluctuations experienced by the two beams in the two arms and obtain two (rather than one) “two-way” measurements. This “data redundancy” allows us to cancel the laser phase noise in the data while retaining a possibly present gravitational wave signal. This is done by properly time-shifting and linearly combining in digital form the two two-way phase differences.



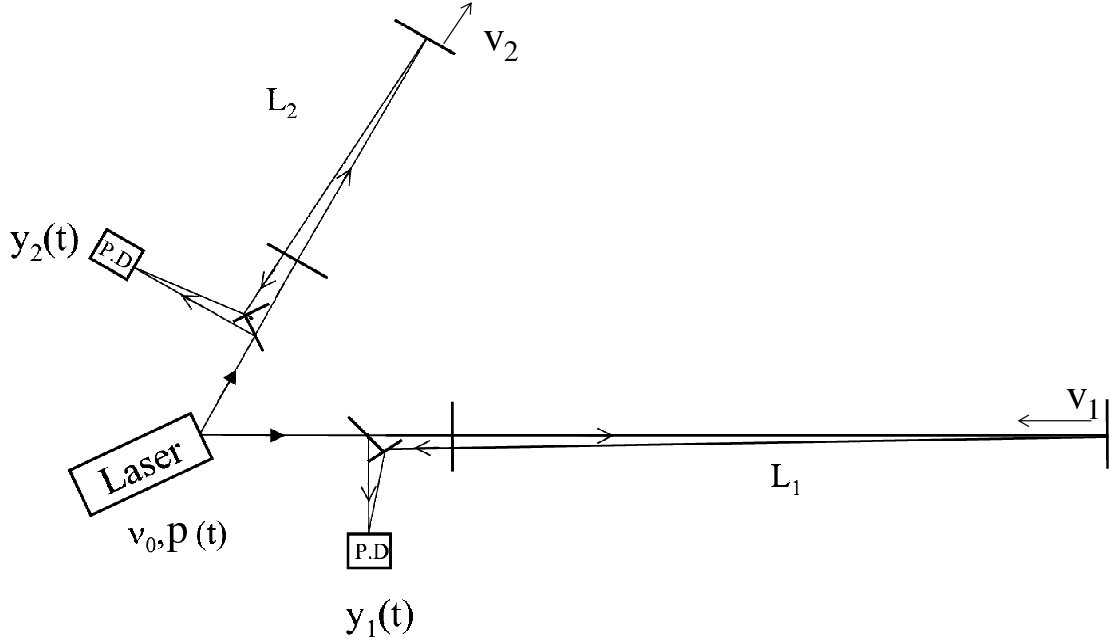


FIG. 2: Light from a laser is split into two beams, each injected into an arm formed by pairs of mirrors moving with velocities  $V_1$  and  $V_2$  relative to the inertial reference frame with respect to which the laser and the beam-splitter are at rest. Since the length of the two arms,  $L_1$  and  $L_2$ , are different, the light beams from the two arms are not recombined at one photo detector. Instead each is separately made to interfere with the light that is injected into the arms. Two distinct photo detectors are now used, and phase (or frequency) fluctuations are then monitored and recorded there. See text for details.

result of this “down-conversion” operation, the two-way data assume the following forms <sup>2</sup>

$$\phi_1(t) = [\nu_0(1 - 2V_1) - \nu_0 - a_1 f]t + p(t - 2L_1) - p(t) - a_1 q(t) + h_1(t) + n_1(t), \quad (1)$$

$$\phi_2(t) = [\nu_0(1 - 2V_2) - \nu_0 - a_2 f]t + p(t - 2L_2) - p(t) - a_2 q(t) + h_2(t) + n_2(t), \quad (2)$$

where  $a_1$ ,  $a_2$  are selected by the NCO in such a way to suppress the beat-notes from the

<sup>2</sup> Throughout this article the speed of light  $c$  and  $2\pi$  are assumed to be equal to 1

two phase measurements to a required value,  $f$  is the microwave frequency generated by the clock driving the down-conversion,  $h_1, h_2$  are the contributions from a possibly present gravitational wave signal, and  $n_1, n_2$  are the random processes associated to the overall remaining noises affecting the two phase measurements. Note that in Eqs. (1, 2) we have denoted with  $q(t)$  the random process associated with the phase noise from the clock driving the NCO [8] and  $p(t)$  the laser noise. Since the coefficients  $a_i, i = 1, 2$  can be made to be equal to  $a_i = -2V_i\nu_0/f, i = 1, 2$ , then Eqs. (1, 2) become

$$\phi_1(t) = p(t - 2L_1) - p(t) - a_1q(t) + h_1(t) + n_1(t) , \quad (3)$$

$$\phi_2(t) = p(t - 2L_2) - p(t) - a_2q(t) + h_2(t) + n_2(t) , \quad (4)$$

If we now assume the clock frequency  $f$  to be the result of implementing a self-referenced OFC that is driven by the onboard laser, then the following relationship between the phase fluctuations of the local oscillator,  $q(t)$ , and those of the laser,  $p(t)$ , holds

$$q(t) = \frac{f}{\nu_0} p(t) + \Delta q(t) . \quad (5)$$

In Eq. (12) we have denoted with  $\Delta q(t)$  the residual noise representing the level of coherence between the frequency of the laser and the microwave frequency referenced to it. It has been demonstrated experimentally [22] that the magnitude of this residual phase noise can be reduced to a level corresponding to an Allan standard deviation of a few parts in  $10^{-19}$  over time scales of interest to space-based GW interferometers. Since this value is three orders of magnitude smaller than the USO noise level required for avoiding the use of the calibration procedure based on modulated beams [8], we can then safely disregard it in our analysis. After substituting Eq. (5) into Eqs. (3, 4) we obtain the expressions for the two-way phase differences when the OFC technique is implemented

$$\phi_1(t) = p(t - 2L_1) - p(t) + 2V_1p(t) + h_1(t) + n_1(t) , \quad (6)$$

$$\phi_2(t) = p(t - 2L_2) - p(t) + 2V_2p(t) + h_2(t) + n_2(t) . \quad (7)$$

Following [26] it is then straightforward to show that the following combination of the two two-way phase measurements cancels the laser noise

$$X^{OFC}(t) \equiv [\phi_1(t - 2L_2) - (1 - 2V_2)\phi_1(t)] - [\phi_2(t - 2L_1) - (1 - 2V_1)\phi_2(t)] . \quad (8)$$

In other words, all  $p(t)$  and  $q(t)$  terms (through Eq. 5) drop out in  $X^{OFC}$ . Although the above expression of the unequal-arm Michelson TDI combination reflects the assumption

that the velocities of the mirrors are large enough to require the removal of the beat-notes from the two-way data but small enough to treat the arm-lengths as constant, it shows that the implementation of the OFC technique allows us to simultaneously cancel the laser and microwave noises with TDI. In the following sections we will remove the assumption of constant arm-lengths and derive the TDI expressions that account for the rotation of the array (Sagnac effect) as well as the time-dependence (“flexi”) of its arms [16, 18, 19].

## B. Generalized TDI formulation

In order to derive the new TDI combinations valid when the OFC technique is used for generating a microwave signal coherent to the onboard laser, we will follow the description of a space-based interferometer (such as LISA and eLISA/NGO with its three operational arms [5–7]) adopted in earlier publications (see reference [19] and references therein).

As shown in Figure 3, where the overall geometry of the interferometer is defined, there are three spacecraft, six optical benches, six lasers, six proof-masses, and twelve photo detectors. There are also six phase difference data going clock-wise and counter-clock-wise around the triangle. The spacecraft are labeled 1, 2, 3 and the optical paths traveled by the light beams as they propagate along the arms of the constellation are denoted  $L_i$  and  $L_{i'}$ , with  $i = 1, 2, 3$  being opposite spacecraft  $i$ . The two optical paths along the same arm are different because the rotational motion of the array results into a difference of the light travel times in the two directions around a Sagnac circuit [16, 27]. As shown in Figure 3 we have conventionally denoted with  $L_{i'}$  and  $L_i$  the optical delays for clockwise and counter-clock-wise propagation respectively. Furthermore, since  $L_i$  and  $L_{i'}$  not only differ from one another but can be time dependent (they “flex”), new second-generation TDI combinations were derived in order to account for this effect. This was done by using the non-commuting time-delay operators formalism discussed in [19], and we will rely on it for the derivation of the new second-generation TDI combinations that simultaneously cancel the noises of the microwave signals generated by the OFC technique.

In Figure 3 the vertices 1, 2, 3 are oriented clockwise, while the unit vectors between spacecraft are denoted  $\hat{n}_i$ , oriented as indicated in the figure. We index the phase difference data to be analyzed as follows: the beam arriving at spacecraft  $i$  has subscript  $i$  and is primed or unprimed depending on whether the beam is traveling clockwise or counter-clockwise (the

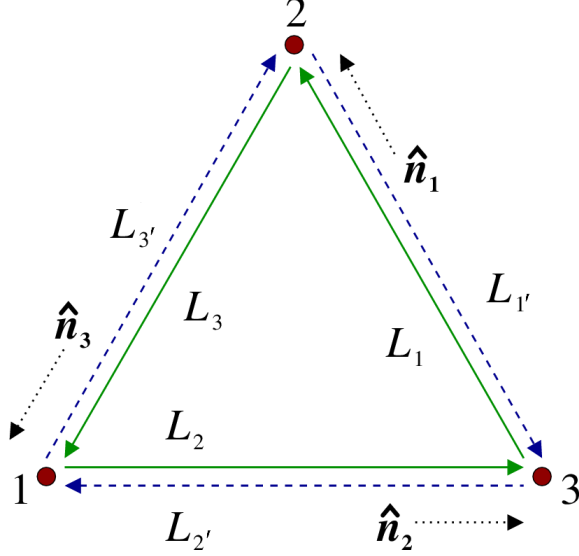


FIG. 3: Schematic array configuration. The spacecraft are labeled 1, 2, and 3. The optical paths are denoted by  $L_i, L_{i'}$  where the index  $i$  corresponds to the opposite spacecraft. The unit vectors  $\hat{n}_i$  point between pairs of spacecraft, with the orientation indicated.

sense defined here with reference to Figure 3) around the triangle, respectively. Thus, as seen from the figure,  $s_1$  is the phase difference time series measured at reception at spacecraft 1 with transmission from spacecraft 2 (along  $L_3$ ).

Similarly,  $s_{1'}$  is the phase difference series derived from reception at spacecraft 1 with transmission from spacecraft 3. The other four one-way phase difference time series from signals exchanged between the spacecraft are obtained by cyclic permutation of the indices:  $1 \rightarrow 2 \rightarrow 3 \rightarrow 1$ . We also adopt the notation for delayed data streams described in [19], in which there are six time-delay operators  $\mathcal{D}_i, \mathcal{D}_{i'}$ ,  $i = 1, 2, 3$ , and where, for any data stream  $\Psi(t)$ ,

$$\mathcal{D}_i \Psi(t) = \Psi(t - L_i), \quad \mathcal{D}_{i'} \Psi(t) = \Psi(t - L_{i'}). \quad (9)$$

For example,  $\mathcal{D}_2 s_1(t) = s_1(t - L_2)$ ,  $\mathcal{D}_{2'} \mathcal{D}_{3'} s_1(t) = s_1(t - L_{3'}(t - L_{2'}) - L_{2'}(t))$ , etc. Note that the operators do not commute, as:  $\mathcal{D}_{3'} \mathcal{D}_{2'} s_1(t) = s_1(t - L_{2'}(t - L_{3'}) - L_{3'}(t)) \neq \mathcal{D}_{2'} \mathcal{D}_{3'} s_1(t) = s_1(t - L_{3'}(t - L_{2'}) - L_{2'}(t))$ .

Following [8], the heterodyne phase measurements,  $s_i(t), s_{i'}$ ,  $i = 1, 2, 3$  can be written in the following form

$$\begin{aligned}
s_1(t) &= [\nu_{2'}(1 - \dot{L}_3) - \nu_1 - a_1 f_1]t + \mathcal{D}_3 p_{2'} - p_1(t) - a_1 q_1(t) + s_1^{gw}(t) + N_1(t) , \\
s_{1'}(t) &= [\nu_3(1 - \dot{L}_{2'}) - \nu_{1'} - a_{1'} f_{1'}]t + \mathcal{D}_{2'} p_3 - p_{1'}(t) - a_{1'} q_{1'}(t) + s_{1'}^{gw}(t) + N_{1'}(t) , \quad (10)
\end{aligned}$$

where we have denoted with  $p_i, p_{i'}$  the lasers phase fluctuations, the microwave frequencies  $f_1, f_{1'}$  are generated by the OFCs driven by lasers 1 and 1' respectively, and the coefficients  $a_1, a_{1'}$  are synthesized by a numerically-controlled oscillator (NCO) to be equal to the following values [8]

$$a_1 = \frac{\nu_{2'}(1 - \dot{L}_3) - \nu_1}{f_1} , \quad a_{1'} = \frac{\nu_3(1 - \dot{L}_{2'}) - \nu_{1'}}{f_{1'}} . \quad (11)$$

In Eq. (10) we have denoted with  $N_1, N_{1'}$  all the remaining noises affecting the one-way measurements, and with  $s_1^{gw}, s_{1'}^{gw}$  the contribution to the one-way Doppler measurements from a passing gravitational wave signal.

Consistently with earlier work [8], Eqs. (10) reflect the assumption of having the frequencies of the lasers different from each other. Note that the phase fluctuations from the microwave frequency references driving the NCO enter into  $s_1$  and  $s_{1'}$  through the terms  $a_1 q_1$  and  $a_{1'} q_{1'}$  respectively. Since these phase fluctuations associated to the microwave signals have been generated by the frequency comb subsystems, they are related to the laser phase fluctuations,  $p_1$  and  $p_{1'}$ , through the following relationships

$$q_1(t) = \frac{f_1}{\nu_1} p_1(t) + \Delta q_1(t) , \quad q_{1'}(t) = \frac{f_{1'}}{\nu_{1'}} p_{1'}(t) + \Delta q_{1'}(t) . \quad (12)$$

In Eq. (12) we have denoted with  $\Delta q_1(t), \Delta q_{1'}(t)$  the residual noises representing the level of coherence between the frequencies of the lasers and the microwave frequencies referenced to them. The magnitude of this residual phase noise has been demonstrated experimentally [22] to correspond to an Allan standard deviation of a few parts in  $10^{-19}$  over time scales of interest to space-based GW interferometers. Since this is three orders of magnitude smaller than the USO noise required for avoiding the use of the calibration procedure based on modulated beams [8], we infer that the contribution from the noises  $\Delta q_i, \Delta q_{i'}, i = 1, 2, 3$  to the overall noise budget of the TDI combinations can be regarded as negligible. For this reason from now on they will be disregarded in our analysis.

If we now substitute Eqs.(11, 12) into Eq.(10), the heterodyne measurements  $s_1, s_{1'}$

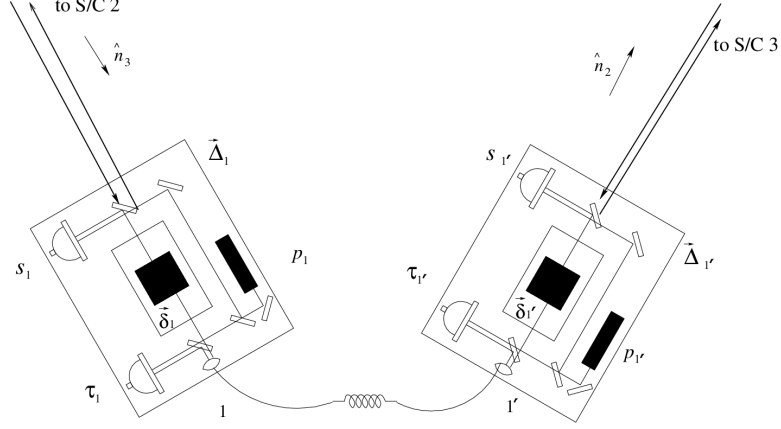


FIG. 4: Schematic diagram of proof-masses-plus-optical-benches onboard the spacecraft. The left-hand bench reads out the phase signals  $s_1$  and  $\tau_1$ . The right-hand bench analogously reads out  $s_{1'}$  and  $\tau_{1'}$ . The random displacements of the two proof masses and two optical benches are indicated (lower case  $\vec{\delta}_i, \vec{\delta}_{i'}$  for the proof masses, upper case  $\vec{\Delta}_i, \vec{\Delta}_{i'}$  for the optical benches).

assume the following forms

$$\begin{aligned} s_1(t) &= \mathcal{D}_3 p_{2'} - p_1(t) - A_1 p_1(t) + s_1^{gw}(t) + N_1(t) , \\ s_{1'}(t) &= \mathcal{D}_2 p_3 - p_{1'}(t) - A_{1'} p_{1'}(t) + s_{1'}^{gw}(t) + N_{1'}(t) , \end{aligned} \quad (13)$$

where the coefficient  $A_1$ ,  $A_{1'}$  are equal to

$$A_1 \equiv \frac{a_1 f_1}{\nu_1} = \frac{\nu_{2'}(1 - \dot{L}_3) - \nu_1}{\nu_1} , \quad A_{1'} \equiv \frac{a_{1'} f_{1'}}{\nu_{1'}} = \frac{\nu_3(1 - \dot{L}_{2'}) - \nu_{1'}}{\nu_{1'}} . \quad (14)$$

Note that, over periods of a few light-times, the coefficients  $A_i$ ,  $A_{i'}$  ( $i = 1, 2, 3$ ) can be regarded as constant since the spacecraft relative velocities start to display a noticeable change only over periods of weeks to months [28].

If we assume the optical bench design to be as shown in Figure 4, then six more phase difference series result from laser beams exchanged between adjacent optical benches within each spacecraft; these are similarly indexed as  $\tau_i, \tau_{i'}$ ,  $i = 1, 2, 3$ .<sup>3</sup> The photo receivers that generate the data  $s_1, s_{1'}, \tau_1$ , and  $\tau_{1'}$  at spacecraft 1 are also shown in figure 4.

<sup>3</sup> The optical bench design shown in figure 4 represents one of the possible configurations for integrating the onboard drag-free system with the heterodyne measurements. Although other optical bench designs result into different inter-proof-mass phase measurements [6, 29], the resulting expressions for the new TDI combinations derived in this article are all equivalent.

The adopted optical bench design shows optical fibers transmitting signals both ways between adjacent benches. We ignore time-delay effects for these signals and will simply denote by  $\mu_i(t)$  the phase fluctuations upon transmission through the fibers of the laser beams with frequencies  $\nu_i$ , and  $\nu_{i'}$ . The  $\mu_i(t)$  phase shifts within a given spacecraft might not be the same for large frequency differences  $\nu_i - \nu_{i'}$ . For the envisioned frequency differences (a few hundred MHz), however, the remaining fluctuations due to the optical fiber can be assumed to be independent of the direction of light propagation through them [30].

If we limit our attention only to the terms containing the laser phase noises, we can then write down the following expressions for the  $\tau_i, \tau_{i'}$  phase measurements

$$\tau_1(t) = [\nu_{1'} - \nu_1 - c_1 f_1]t + p_{1'}(t) - p_1(t) - c_1 \frac{f_1}{\nu_1} p_1(t) , \quad (15)$$

$$\tau_{1'}(t) = [\nu_1 - \nu_{1'} - c_{1'} f_{1'}]t + p_1(t) - p_{1'}(t) - c_{1'} \frac{f_{1'}}{\nu_{1'}} p_{1'}(t) , \quad (16)$$

where, like in the case of the inter-spacecraft measurements  $s_1, s_{1'}$ , the coefficient  $c_1, c_{1'}$  are determined by the NCO to be equal to

$$c_1 = \frac{\nu_{1'} - \nu_1}{f_1} , \quad c_{1'} = \frac{\nu_1 - \nu_{1'}}{f_{1'}} . \quad (17)$$

Note that in Eq. (17) we have used the relationship between the phase noise of the microwave signal and that of its driving laser (Eq. (12)). As discussed in other TDI references [8, 19] the inter-bench phase measurements  $\tau_i, \tau_{i'}$  enter into the TDI combinations in the form of their differences. It is therefore convenient to rewrite the set of heterodyne measurements in the following form (for simplicity of notation we will omit the contribution from the gravitational wave signal and the other noises in the  $s_1$  and  $s_{1'}$  measurements)

$$s_1 = \mathcal{D}_3 p_{2'} - (1 + A_1) p_1 , \quad (18)$$

$$s_{1'} = \mathcal{D}_2 p_3 - (1 + A_{1'}) p_{1'} , \quad (19)$$

$$z_1 \equiv \frac{\tau_1 - \tau_{1'}}{2} = (1 + \frac{\rho_{1'}}{2}) p_{1'} - (1 + \frac{\rho_1}{2}) p_1 , \quad (20)$$

where  $\rho_1, \rho_{1'}$ , are equal to

$$\rho_1 \equiv \frac{\nu_{1'} - \nu_1}{\nu_1} , \quad \rho_{1'} = \frac{\nu_1 - \nu_{1'}}{\nu_{1'}} . \quad (21)$$

Six other relations, for the readouts at vertices 2 and 3, are given by cyclic permutation of the indices in Eqs. (18, 19, 20).

In order to derive the new TDI combinations that rely on the OFC technique, we will start by taking specific combinations of the one-way data entering in each of the expressions derived above. Following the approach in [18, 19], these combinations are identified by requiring the laser noises entering into them to be only of one “kind”, i.e. with primed or unprimed indeces. After some simple algebra to account for the presence of the heterodyne coefficients, these combinations of the one-way heterodyne measurements (called  $\eta_i$ ,  $\eta_{i'}$  in [19]) here assume the following forms

$$\eta_1 \equiv \frac{1 + \frac{\rho_{2'}}{2}}{1 + \frac{\rho_2}{2}} s_1 - \frac{D_3 z_2}{1 + \frac{\rho_2}{2}} = \mathcal{D}_3 p_2 - I_1 p_1, \quad (22)$$

$$\eta_{1'} \equiv s_{1'} + \frac{1 + A_{1'}}{1 + \frac{\rho_{1'}}{2}} z_1 = \mathcal{D}_{2'} p_3 - I_{1'} p_1, \quad (23)$$

where the coefficients  $I_1$ ,  $I_{1'}$  are given by the following expressions

$$I_1 \equiv \frac{(1 + A_{1'})(1 + \frac{\rho_1}{2})}{1 + \frac{\rho_{1'}}{2}}, \quad I_{1'} \equiv \frac{(1 + A_1)(1 + \frac{\rho_{2'}}{2})}{1 + \frac{\rho_2}{2}}, \quad (24)$$

and the other  $\eta$ -combinations are obtained as usual by permutations of the spacecraft indeces.

The new TDI combinations are chosen in such a way so as to retain only one of the three noises  $p_i$ ,  $i = 1, 2, 3$ , if possible. In this way we can then implement an iterative procedure based on the use of these basic combinations and of time-delay operators, to cancel the laser noises after dropping terms that are quadratic in  $\dot{L}/c$  or linear in the accelerations [16, 18, 19]. This iterative time-delay method, to first order in the velocity, is illustrated abstractly as follows. Given a function of time  $\Psi = \Psi(t)$ , time delay by  $L_i$  is now denoted either with the standard comma notation [31] or by applying the delay operator  $\mathcal{D}_i$ ,

$$\mathcal{D}_i \Psi = \Psi_{,i} \equiv \Psi(t - L_i(t)). \quad (25)$$

We then impose a second time delay  $L_j(t)$ :

$$\begin{aligned} \mathcal{D}_j \mathcal{D}_i \Psi &= \Psi_{;ij} \equiv \Psi(t - L_j(t) - L_i(t - L_j(t))) \\ &\simeq \Psi(t - L_j(t) - L_i(t) + \dot{L}_i(t) L_j) \\ &\simeq \Psi_{,ij} + \dot{\Psi}_{,ij} \dot{L}_i L_j. \end{aligned} \quad (26)$$



A third time delay  $L_k(t)$  gives

$$\begin{aligned} \mathcal{D}_k \mathcal{D}_j \mathcal{D}_i \Psi &= \Psi_{;ijk} = \Psi(t - L_k(t) - L_j(t - L_k(t)) - L_i(t - L_k(t) - L_j(t - L_k(t)))) \\ &\simeq \Psi_{,ijk} + \dot{\Psi}_{,ijk} \left[ \dot{L}_i(L_j + L_k) + \dot{L}_j L_k \right], \end{aligned} \quad (27)$$

and so on, recursively; each delay generates a first-order correction proportional to its rate of change times the sum of all delays coming after it in the subscripts. Commas have now been replaced with semicolons [17], to remind us that we consider moving arrays. When the sum of these corrections to the terms of a data combination vanishes, the combination is called flex-free. Finally, it should be noticed that each delay operator,  $\mathcal{D}_i$  has a unique inverse operator,  $\mathcal{D}_i^{-1}$ , whose expression can be derived by requiring that  $\mathcal{D}_i^{-1} \mathcal{D}_i = I$  and neglecting quadratic and higher-order velocity terms. Its action to a time series  $\Psi(t)$  is

$$\mathcal{D}_i^{-1} \Psi(t) \equiv \Psi(t + L_i(t + L_i)), \quad (28)$$

i.e. it advances the time-series by a delay  $L_i$  estimated not at time  $t$  but rather at time  $t + L_i$ .

### C. The unequal-arm Michelson

The unequal-arm Michelson combination synthesized onboard spacecraft # 1 relies on the four measurements  $\eta_1$ ,  $\eta_{1'}$ ,  $\eta_{2'}$ , and  $\eta_3$ . From Eqs. (22, 23), after some simple algebra, it is easy to show that the following two combinations,  $I_{2'}\eta_1 + D_3\eta_{2'}$  and  $I_3\eta_{1'} + D_2\eta_3$ , contain only the noise from laser # 1 and have the following forms

$$I_{2'}\eta_1 + \eta_{2';3} = (\mathcal{D}_3 \mathcal{D}_{3'} - I_1 I_{2'}) p_1, \quad (29)$$

$$I_3\eta_{1'} + \eta_{3;2'} = (\mathcal{D}_{2'} \mathcal{D}_2 - I_{1'} I_3) p_1. \quad (30)$$

Since in the quasi-stationary case any pairs of these operators commute, i.e.,  $\mathcal{D}_i \mathcal{D}_{j'} - \mathcal{D}_{j'} \mathcal{D}_i \approx 0$ , from Eqs. (29 and 30) it is easy to derive the following expression for the unequal-arm interferometric combination  $X^{OFC}$  that eliminates  $p_1$ :

$$X^{OFC} = [\mathcal{D}_{2'} \mathcal{D}_2 - I_{1'} I_3] (I_{2'}\eta_1 + \eta_{2';3}) - [(\mathcal{D}_3 \mathcal{D}_{3'} - I_1 I_{2'})] (I_3\eta_{1'} + \eta_{3;2'}). \quad (31)$$

If, on the other hand, the time-dependence of the delays is such as to prevent the delay operators to commute, the expression of the unequal-arm Michelson combination above no longer

cancels  $p_1$ . In order to derive the new expression for the unequal-arm interferometer that accounts for “flexing” and simultaneously cancels the noise from the microwave frequency signal referenced to the onboard lasers, let us first consider the following two combinations of the one-way measurements entering into the  $X^{OFC}$  observable given in Eq. (31):

$$[I_1 I_{2'} (I_3 \eta_{1'} + \eta_{3;2'}) + (I_{2'} \eta_1 + \eta_{2';3});_{22'}] = [D_{2'} D_2 D_3 D_{3'} - I_1 I_{1'} I_{2'} I_3] p_1 , \quad (32)$$

$$[I_{1'} I_3 (I_{2'} \eta_1 + \eta_{2';3}) + (I_3 \eta_{1'} + \eta_{3;2'})_{;3'3}] = [D_3 D_{3'} D_{2'} D_2 - I_1 I_{1'} I_{2'} I_3] p_1 . \quad (33)$$

Using Equations (32, 33) we can use the “delay technique” again to finally derive the following expression for the new unequal-arm Michelson combination  $X_1^{OFC}$ . This new TDI combination accounts for the flexing effect and cancels the noise of the microwave signal referenced to the laser frequency through the OFC technique

$$\begin{aligned} X_1^{OFC} = & [D_{2'} D_2 D_3 D_{3'} - I_1 I_{1'} I_{2'} I_3] [I_{1'} I_3 (I_{2'} \eta_1 + \eta_{2';3}) + (I_3 \eta_{1'} + \eta_{3;2'})_{;3'3}] \\ & - [D_3 D_{3'} D_{2'} D_2 - I_1 I_{1'} I_{2'} I_3] [I_1 I_{2'} (I_3 \eta_{1'} + \eta_{3;2'}) + (I_{2'} \eta_1 + \eta_{2';3});_{22'}] . \end{aligned} \quad (34)$$

As usual,  $X_2^{OFC}$  and  $X_3^{OFC}$  are obtained by cyclic permutation of the spacecraft indices. This expression is readily shown to be laser-noise-free to first order of spacecraft separation velocities  $\dot{L}_i$  (it is “flex-free”) and it simultaneously removes the phase noise from the microwave signal (generated by the OFC technique) used in the heterodyne measurements.

#### D. The Sagnac combinations

In the case of the Sagnac variables  $(\alpha, \beta, \gamma, \zeta)$  [19] light originating from a spacecraft is simultaneously sent around the array on clockwise and counter-clockwise loops, and the two returning beams are then recombined. If the array is rotating and flexing, the two beams experience a different delay due to the rotation of the array (the Sagnac effect) as well as the time-dependence of the armlengths and the resulting Doppler effects.

Since the previously derived Sagnac TDI combinations no longer simultaneously cancel the laser and the microwave signal noises, in order to derive the new TDI expressions let us first write down the six terms entering, for instance, into the  $\alpha$  combination suitable for a stationary array (see equation (60) in [19]) in the attempt to explicitly identify the expression of the new TDI combination,  $\alpha^{OFC}$ . This combination must satisfy the property of removing the same laser fluctuations affecting two beams that have been made to propagated

clockwise and counter-clockwise around the array. The expression for  $\alpha$  (equation (60) of [19]) contains six terms, i.e.  $\eta_{1'}, \mathcal{D}_{2'}\eta_{3'}, \mathcal{D}_{1'}\mathcal{D}_{2'}\eta_{2'}, \eta_1, \mathcal{D}_3\eta_2, \mathcal{D}_1\mathcal{D}_3\eta_3$ , which now assume the following forms

$$\eta_{1'} = \mathcal{D}_{2'}p_3 - I_{1'}p_1, \quad (35)$$

$$\mathcal{D}_{2'}\eta_{3'} = \mathcal{D}_{2'}\mathcal{D}_{1'}p_2 - I_{3'}\mathcal{D}_{2'}p_3, \quad (36)$$

$$\mathcal{D}_{1'}\mathcal{D}_{2'}\eta_{2'} = \mathcal{D}_{1'}\mathcal{D}_{2'}\mathcal{D}_{3'}p_1 - I_{2'}\mathcal{D}_{1'}\mathcal{D}_{2'}p_2, \quad (37)$$

$$\eta_1 = \mathcal{D}_3p_2 - I_1p_1, \quad (38)$$

$$\mathcal{D}_3\eta_2 = \mathcal{D}_3\mathcal{D}_1p_3 - I_2\mathcal{D}_3p_2, \quad (39)$$

$$\mathcal{D}_3\mathcal{D}_1\eta_3 = \mathcal{D}_3\mathcal{D}_1\mathcal{D}_2p_1 - I_3\mathcal{D}_3\mathcal{D}_1p_3. \quad (40)$$

By simple inspection of the above expressions it is easy to see that the following two linear combinations of the above six measurements only contain the laser noise  $p_1$

$$\alpha_{\uparrow} \equiv I_2I_3'\eta_{1'} + I_2'\mathcal{D}_{2'}\eta_{3'} + \mathcal{D}_{1'}\mathcal{D}_{2'}\eta_{2'} = [\mathcal{D}_{1'}\mathcal{D}_{2'}\mathcal{D}_{3'} - I_1'I_2'I_3']p_1, \quad (41)$$

$$\alpha_{\downarrow} \equiv I_2I_3\eta_1 + I_3\mathcal{D}_3\eta_2 + \mathcal{D}_3\mathcal{D}_1\eta_3 = [\mathcal{D}_3\mathcal{D}_1\mathcal{D}_2 - I_1I_2I_3]p_1. \quad (42)$$

Since the delay operators do not commute, we conclude that the straight difference  $\alpha_{\uparrow} - \alpha_{\downarrow}$  does not cancel the laser noise. However, if we now apply the ‘‘delay technique’’ [18, 19] to the combinations given in Eqs. (41, 42) we finally get the expression for the Sagnac combination  $\alpha_1^{OFC}$

$$\alpha_1^{OFC} \equiv [\mathcal{D}_3\mathcal{D}_1\mathcal{D}_2 - I_1I_2I_3]\alpha_{\uparrow} - [\mathcal{D}_{1'}\mathcal{D}_{2'}\mathcal{D}_{3'} - I_1'I_2'I_3']\alpha_{\downarrow}, \quad (43)$$

Although the combination  $\alpha_1^{OFC}$  still shows the presence of a residual laser noise, it can be shown to be small as it involves the difference of the clockwise and counter-clockwise rates of change of the propagation delays on the *same* circuit. For LISA, the remaining laser phase noises in  $\alpha_i^{OFC}$ ,  $i = 1, 2, 3$ , are several orders of magnitude below the secondary noises.

In order to derive the new TDI expression for the fully symmetric Sagnac combination,  $\zeta$ , we remind the reader that the rotation of the array breaks the symmetry and therefore its uniqueness. However, there still exist three generalized TDI laser-noise-free data combinations that have properties very similar to  $\zeta$ , and which can be used for the same scientific purposes [32]. These combinations, which we call  $(\zeta_1^{OFC}, \zeta_2^{OFC}, \zeta_3^{OFC})$ , can be derived by applying again our time-delay operator approach.

In order to proceed with the derivation of  $\zeta_1^{OFC}$ , we should first remind ourselves that this TDI combination contains all six  $\eta_i, \eta_{i'}$ ,  $i = 1, 2, 3$ , each of which is delayed only once [31]. By simple inspection of the TDI combination  $\zeta_1$  given in Eq. (67) of reference [19], we will start by considering the following six terms entering in it

$$\begin{aligned}
\eta_{3,3} &= \mathcal{D}_3 \mathcal{D}_2 p_1 - I_3 \mathcal{D}_3 p_3 , \\
\eta_{3',3} &= \mathcal{D}_3 \mathcal{D}_{1'} p_2 - I_{3'} \mathcal{D}_3 p_3 , \\
\eta_{1,1'} &= \mathcal{D}_{1'} \mathcal{D}_3 p_2 - I_1 \mathcal{D}_{1'} p_1 , \\
\eta_{1',1} &= \mathcal{D}_1 \mathcal{D}_{2'} p_3 - I_{1'} \mathcal{D}_1 p_1 , \\
\eta_{2,2'} &= \mathcal{D}_{2'} \mathcal{D}_1 p_3 - I_2 \mathcal{D}_{2'} p_2 , \\
\eta_{2',2'} &= \mathcal{D}_{2'} \mathcal{D}_{3'} p_1 - I_{2'} \mathcal{D}_{2'} p_2 .
\end{aligned} \tag{44}$$

If the array is rigidly rotating (i.e. its arm lengths are constant), it is easy to see that the following combinations contain only the noise from laser # 1

$$I_3 \eta_{1,1'} - I_3 \eta_{3',3} + I_{3'} \eta_{3,3} = [I_{3'} \mathcal{D}_3 \mathcal{D}_2 - I_1 I_3 \mathcal{D}_{1'}] p_1 , \tag{45}$$

$$I_{2'} \eta_{1',1} - I_2 \eta_{2,2'} + I_2 \eta_{2',2'} = [I_2 \mathcal{D}_{2'} \mathcal{D}_{3'} - I_{1'} I_2 \mathcal{D}_1] p_1 , \tag{46}$$

as we have used the commutativity property of the delay operators in order to cancel the  $p_2$  and  $p_3$  terms. Since both sides of the two equations above contain only the  $p_1$  noise,  $\zeta_1^{OFC}$  is found by the following expression:

$$\begin{aligned}
\zeta_1^{OFC} &= [I_2 \mathcal{D}_{2'} \mathcal{D}_{3'} - I_{1'} I_2 \mathcal{D}_1] (I_3 \eta_{1,1'} - I_3 \eta_{3',3} + I_{3'} \eta_{3,3}) \\
&\quad - [I_{3'} \mathcal{D}_3 \mathcal{D}_2 - I_1 I_3 \mathcal{D}_{1'}] (I_{2'} \eta_{1',1} - I_2 \eta_{2,2'} + I_2 \eta_{2',2'}) ,
\end{aligned} \tag{47}$$

which is a generalization of Eq. (67) given in [19]. If the delay-times also change in time, the perfect cancellation of the laser noises is no longer achieved in the  $(\zeta_1^{OFC}, \zeta_2^{OFC}, \zeta_3^{OFC})$  combinations derived above. However, following the considerations made for the corresponding second-generation TDI combinations derived in [18], it can be shown that for a mission like LISA the magnitude of the residual laser noises in these combinations are significantly smaller than the secondary system noises, making their effects entirely negligible.

### E. The Monitor, Beacon, and Relay Combinations

The expressions of the Relay ( $U_1^{OFC}$ ), Beacon ( $P_1^{OFC}$ ), and Monitor ( $E_1^{OFC}$ ) combinations that account for the rotation, flexing of the array, and implementation of the OFC technique, can also be derived by applying the time-delay iterative procedure highlighted in the previous subsections. However, as also noted in [18], in order to reduce the number of terms in the monitor combinations we will rely on the use of the inverse delay operator  $D_i^{-1}$ ,  $D_{i'}^{-1}$ ,  $i = 1, 2, 3$ .

#### 1. The relay

In a *relay* combination,  $U_1^{OFC}$ , one spacecraft is capable of only receiving a laser beam along one arm and transmitting along the other. If, for instance, we take spacecraft # 1 to be the relay spacecraft, the resulting TDI combination may contain the following four measurements [18]:  $\eta_{1'}$ ,  $\eta_2$ ,  $\eta_{2'}$ ,  $\eta_{3'}$ . If we now consider the expressions given in Eqs. (44-45) derived in [18] for the relay combination without OFC, it is relatively easy to obtain from them the following equivalent expressions valid when the OFC technique is implemented

$$I_{1'}I_2I_{3'}\eta_{2'} + I_2I_{3'}\eta_{1',3'} + I_2\eta_{3';2'3'} + \eta_{2;1'2'3'} - I_{1'}I_2I_{3'}\eta_2 = [\mathcal{D}_{3'}\mathcal{D}_{2'}\mathcal{D}_{1'} - I_{1'}I_2I_{3'}]\mathcal{D}_1p_3 \quad (48)$$

$$I_{1'}\eta_{2';1'1} + I_{1'}I_2\eta_{3',1} + \eta_{1';3'1'1} = \mathcal{D}_1[\mathcal{D}_{1'}\mathcal{D}_{3'}\mathcal{D}_{2'} - I_{1'}I_2I_{3'}]p_3 \quad (49)$$

By applying the operator  $\mathcal{D}_1[\mathcal{D}_{1'}\mathcal{D}_{3'}\mathcal{D}_{2'} - I_{1'}I_2I_{3'}]$  to the left-hand-side of Eq.(48), the operator  $[\mathcal{D}_{3'}\mathcal{D}_{2'}\mathcal{D}_{1'} - I_{1'}I_2I_{3'}]\mathcal{D}_1$  to the left-hand-side of Eq. (49), and then take the difference of the resulting two expressions, we get the following expression for the second-generation relay combination when OFC is implemented

$$\begin{aligned} U_1^{OFC} &= \mathcal{D}_1[\mathcal{D}_{1'}\mathcal{D}_{3'}\mathcal{D}_{2'} - I_{1'}I_2I_{3'}] \{I_{1'}I_2I_{3'}\eta_{2'} + I_2I_{3'}\eta_{1',3'} + I_2\eta_{3';2'3'} + \eta_{2;1'2'3'} - I_{1'}I_2I_{3'}\eta_2\} \\ &\quad - [\mathcal{D}_{3'}\mathcal{D}_{2'}\mathcal{D}_{1'} - I_{1'}I_2I_{3'}]\mathcal{D}_1 \{I_{1'}\eta_{2';1'1} + I_{1'}I_2\eta_{3',1} + \eta_{1';3'1'1}\} \end{aligned} \quad (50)$$

with  $U_2^{OFC}$ ,  $U_3^{OFC}$  obtained by cycling the spacecraft indices. It can readily be verified that the laser noise remaining in this combination vanishes to first order in the inter-spacecraft velocities.

## 2. The beacon

In the *beacon* combination, say  $P_1^{OFC}$ , spacecraft # 1 transmits (only) to the other two while the other two exchange laser light as usual. In this operating mode only the measurements  $\eta_2$ ,  $\eta_{2'}$ ,  $\eta_3$ ,  $\eta_{3'}$  will be available for synthesizing the combination  $P_1^{OFC}$ . To identify its expression we proceed by modifying Eqs. (49-50) given in [18] in such a way to exactly cancel the  $p_2$ ,  $p_3$  laser noises while retaining  $p_1$ . After some long but straightforward algebra we get the following two expressions that contain only  $p_1$

$$I_2 I_3 \eta_{3',3'} + I_3 \eta_{2;1'3'} + \eta_{3;11'3'} - I_2 I_3' \eta_{3,3'} = \mathcal{D}_{3'}[\mathcal{D}_{1'}\mathcal{D}_1 - I_2 I_3']\mathcal{D}_2 p_1, \quad (51)$$

$$I_2' I_3' \eta_{2,2} + I_2' \eta_{3';12} + \eta_{2';1'12} - I_2' I_3' \eta_{2',2} = \mathcal{D}_2[\mathcal{D}_1\mathcal{D}_{1'} - I_2' I_3']\mathcal{D}_{3'} p_1. \quad (52)$$

By now applying our time-delay iterative procedure we obtain the final expression for  $P_1^{OFC}$

$$\begin{aligned} P_1^{OFC} &= \mathcal{D}_2[\mathcal{D}_1\mathcal{D}_{1'} - I_2 I_3']\mathcal{D}_{3'}[I_2 I_3 \eta_{3',3'} + I_3 \eta_{2;1'3'} + \eta_{3;11'3'} - I_2 I_3' \eta_{3,3'}] \\ &\quad - \mathcal{D}_{3'}[\mathcal{D}_{1'}\mathcal{D}_1 - I_2' I_3']\mathcal{D}_2[I_2' I_3' \eta_{2,2} + I_2' \eta_{3';12} + \eta_{2';1'12} - I_2' I_3' \eta_{2',2}] \end{aligned} \quad (53)$$

## 3. The monitor

In the *monitor* combination,  $E_1^{OFC}$  for instance, spacecraft # 1 receives (only) from the other two while the other two exchange laser light as usual;  $E_1^{OFC}$  therefore relies only on the measurements  $\eta_1$ ,  $\eta_{1'}$ ,  $\eta_2$ ,  $\eta_{3'}$ . If we now consider the expressions given in Eqs. (54-57) of [18] for the monitor combination without OFC, it is relatively easy to derive from them the following equivalent expressions valid when the OFC technique is implemented

$$\eta_{1;11'} - I_2 I_3' \eta_1 = [\mathcal{D}_{1'}\mathcal{D}_1 - I_2 I_3']\mathcal{D}_3 p_2 - I_1[\mathcal{D}_{1'}\mathcal{D}_1 - I_2 I_3']p_1, \quad (54)$$

$$I_3' \eta_{2,3} + \eta_{3';13} = \mathcal{D}_3[\mathcal{D}_1\mathcal{D}_{1'} - I_2 I_3']p_2, \quad (55)$$

$$\eta_{1';1'1} - I_2 I_3' \eta_{1'} = [\mathcal{D}_1\mathcal{D}_{1'} - I_2 I_3']\mathcal{D}_2 p_3 - I_1'[\mathcal{D}_1\mathcal{D}_{1'} - I_2 I_3']p_1, \quad (56)$$

$$I_2 \eta_{3',2'} + \eta_{2;1'2'} = \mathcal{D}_{2'}[\mathcal{D}_{1'}\mathcal{D}_1 - I_2 I_3']p_3. \quad (57)$$

The above expressions can be first combined in pairs to remove the  $p_2$ ,  $p_3$  noises in the following way

$$\begin{aligned} &[\mathcal{D}_{1'}\mathcal{D}_1 - I_2 I_3']\mathcal{D}_3[I_3' \eta_{2,3} + \eta_{3';13}] - \mathcal{D}_3[\mathcal{D}_1\mathcal{D}_{1'} - I_2 I_3'][\eta_{1;11'} - I_2 I_3' \eta_1] \\ &= I_1 \mathcal{D}_3[\mathcal{D}_1\mathcal{D}_{1'} - I_2 I_3'][\mathcal{D}_{1'}\mathcal{D}_1 - I_2 I_3']p_1, \end{aligned} \quad (58)$$

$$\begin{aligned}
& [\mathcal{D}_1 \mathcal{D}_{1'} - I_2 I_{3'}] \mathcal{D}_{2'} [I_2 \eta_{3',2'} + \eta_{2;1'2'}] - \mathcal{D}_{2'} [\mathcal{D}_{1'} \mathcal{D}_1 - I_2 I_{3'}] [\eta_{1';1'1} - I_2 I_{3'} \eta_{1'}] \\
& = I_{1'} \mathcal{D}_{2'} [\mathcal{D}_{1'} \mathcal{D}_1 - I_2 I_{3'}] [\mathcal{D}_1 \mathcal{D}_{1'} - I_2 I_{3'}] p_1 . \quad (59)
\end{aligned}$$

To find the final expression for  $E_1^{OFC}$  we could apply again the iterative procedure. However, to get an expression that has a smaller number of terms [18], we will use the inverse delay operators,  $\mathcal{D}_{2'}^{-1}$ ,  $\mathcal{D}_3^{-1}$ . By simply inspecting the right-hand-sides of Eqs. (58, 59), it is easy to derive the following expression for  $E_1^{OFC}$

$$\begin{aligned}
E_1^{OFC} & = I_{1'} \mathcal{D}_3^{-1} [\mathcal{D}_{1'} \mathcal{D}_1 - I_2 I_{3'}] \mathcal{D}_3 [I_{3'} \eta_{2,3} + \eta_{3';13}] - I_{1'} [\mathcal{D}_1 \mathcal{D}_{1'} - I_2 I_{3'}] [\eta_{1;11'} - I_2 I_{3'} \eta_1] \\
& - I_1 \mathcal{D}_{2'}^{-1} [\mathcal{D}_1 \mathcal{D}_{1'} - I_2 I_{3'}] \mathcal{D}_{2'} [I_2 \eta_{3',2'} + \eta_{2;1'2'}] + I_1 [\mathcal{D}_{1'} \mathcal{D}_1 - I_2 I_{3'}] [\eta_{1';1'1} - I_2 I_{3'} \eta_{1'}] \quad (60)
\end{aligned}$$

which can easily be shown to be laser noise-free to first order in the systematic relative velocities of the spacecraft.

#### IV. SUMMARY AND CONCLUSIONS

We have derived second-generation time-delay interferometric combinations valid when the microwave signal used for heterodyning the phase measurements is generated by an onboard optical-frequency comb subsystem rather than a USO. This provides a microwave signal that is coherent to the frequency of the onboard stabilized laser, and results in a significant simplification of the onboard interferometry system. This is because (i) generation of modulated beams and additional heterodyne measurements involving sidebands are no longer needed, and (ii) the entire onboard USO subsystem can be replaced with the microwave signal referenced to the onboard laser. The corresponding hardware simplification results in a considerably reduced system complexity and probability of subsystem failure. Recent progress in the realization of a space-qualified OFC indicates that such a capability will be available before the planned flight of the ESA gravitational wave mission eLISA [6].

#### Acknowledgments

We acknowledge financial support provided by the Jet Propulsion Laboratory Research & Technology Development program. This research was performed at the Jet Propulsion Laboratory, California Institute of Technology, under contract with the National Aeronautics

and Space Administration.

---

- [1] K.S. Thorne, Gravitational Radiation: Editors S.W. Hawking and W. Israel, (Cambridge University Press, New York, 1987) p. 330.
- [2] J. Weber, *Phys. Rev. Lett.*, **17**, (1966) 1228.
- [3] The LIGO project website can be found at the following URL: <http://www.ligo.caltech.edu/>
- [4] The VIRGO project website can be found at the following URL: <http://www.virgo.infn.it/>
- [5] LISA: Unveiling a hidden Universe, ESA publication # ESA/SRE (2011) 3 (February 2011).  
<http://sci.esa.int/science-e/www/object/index.cfm?fobjectid=48364>
- [6] The eLISA website can be found at the following URL: <https://www.elisascience.org/>
- [7] The NGO website can be found at the following URL: <http://sci.esa.int/ngo/>
- [8] M. Tinto, F.B. Estabrook, and J.W. Armstrong, *Phys. Rev. D*, , **65**, 082003 (2002).
- [9] R.W. Hellings, G. Giampieri, L. Maleki, M. Tinto, K. Danzmann, J. Homes, and D. Robertson, *Opt. Commun.* **124**, 313 (1996).
- [10] R.W. Hellings, *Phys. Rev. D* **64**, 022002 (2001).
- [11] J.L. Hall, *Reviews of Modern Physics*, **78**, 1279 (2006).
- [12] T.W. Hänsch, *Reviews of Modern Physics*, **78**, 1297 (2006).
- [13] T. Wilken, M. Lezius, T. W. Hänsch, A. Kohfeldt, A. Wicht, V. Schkolnik, M. Krutzik, H. Duncker, O. Hellmig, P. Windpassinger, K. Sengstock, A. Peters, and R. Holzwarth, *CLEO: Applications and Technology*, San Jose, California United States June 9-14 (2013).
- [14] J. Lee, K. Lee Y.S. Jang, H. Jang, S. Han, S.H. Lee, K.I. Kang, C.W. Lim, Y.J. Kim, S.W. Kim, *Nature Scientific Reports*, **4**, 5134 (2014).
- [15] T. J. Kippenberg, R. Holzwarth, and S. A. Diddams, *Science*, **332**, 555 (2011).
- [16] N.J. Cornish, and R.W. Hellings, *Class. Quantum Grav.*, **20**, 4851 (2003).
- [17] D.A. Shaddock, M. Tinto, F.B. Estabrook, and J.W. Armstrong, *Phys. Rev. D*, **68**, 061303 (2003).
- [18] M. Tinto, F.B. Estabrook, and J.W. Armstrong, *Phys. Rev. D*, **69**, 082001 (2004).
- [19] M. Tinto, S.V. Dhurandhar, “Time-Delay Interferometry” *Living Rev. Relativ.* **17** (6) (2014).  
<http://relativity.livingreviews.org/Articles/lrr-2014-6/>.
- [20] *Femtosecond Optical Frequency Comb: Principle, Operation, and Applications*, pag. 112, J.



- Ye, S. Cundiff (Eds.), Kluwer Academic Publishing, Norwell, MA (2005).
- [21] J. Reichert, M. Niering, R. Holzwarth, M. Weitz, T. Udem, and T. W. Hänsch, *Phys. Rev. Lett.*, **84**, 3232 (2000).
- [22] L.S. Ma, Z. Bi, A. Bartels, L. Robertsson, M. Zucco, R.S. Windeler, G. Wilpers, C. Oates, L. Hollberg, S.A. Diddams, *Science*, **303**, 1843 (2004).
- [23] T.J. Kippenberg, R. Holzwarth, and S.A. Diddams, *Science* **332**, 555 (2011).
- [24] Y. K. Chembo and N. Yu, *Phys. Rev. A* **82**, 033801 (2010).
- [25] T. Herr, V. Brasch, J. D. Jost, C. Y. Wang, N. M. Kondratiev, M. L. Gorodetsky & T. J. Kippenberg, *Nature Photonics*, **8**, 145152 (2014).
- [26] M. Tinto, & J.W. Armstrong *Phys. Rev. D*, **59**, 102003 (1999).
- [27] D.A. Shaddock, *Phys. Rev. D*, **69**, 022001 (2004).
- [28] W.M. Folkner, F. Hechler, T.H. Sweetser, M.A. Vincent, and P.L. Bender, *Class. Quantum Grav.*, **14**, 1405 (1997).
- [29] Ke-Xun Sun, G. Allen, S. Buchman, D. DeBra, R. Byer, *Class. Quantum Grav.*, **22**, S287 (2005).
- [30] F.B. Estabrook, M. Tinto, & J.W. Armstrong, *Phys. Rev. D*, **62**, 042002 (2000).
- [31] J.W. Armstrong, F.B. Estabrook, & M. Tinto, *Ap. J.*, **527**, 814 (1999).
- [32] M. Tinto, J.W. Armstrong, and F.B. Estabrook, *Phys. Rev. D*, **63**, 021101(R) (2000).